Available online at www.sciencedirect.com

ScienceDirect

Procedia Engineering 81 (2014) 2198 – 2204

Procedia Engineering

www.elsevier.com/locate/procedia

11th International Conference on Technology of Plasticity, ICTP 2014, 19-24 October 2014, Nagoya Congress Center, Nagoya, Japan

Strength and formability designs of tube-hydroformed automotive front sub-frame

Sin-Liang Lin, Bo-Hao Huang, Fuh-Kuo Chen*

Department of Mechanical Engineering, National Taiwan University, Taipei, Taiwan

Abstract

To call for carbon cut, the automobile industry has been widely used tube-hydroforming technology instead of traditional stamping technology to achieve the reduction of structural weight, the enhancement of vehicle structural strength and low fuel consumption. This study targets on automobile front suspension system in modifying the front sub-frame design from stamping-welding parts to a one-piece tube-hydroformed part. First of all, this study refers to the result of cross-section analysis to put up with the modification directions to meet the part strength and manufacturability requirements. According to the modified finished surface, the part strength was evaluated by the comparing the stress and strain distributions of the tube-hydroformed part with those of stamping-welding parts. The impact properties of the tube-hydroformed part was also examined and the results indicated that the tube-hydroformed part exhibits a satisfactory impact mechanism and better capability in energy absorption compared to the stamping-welding parts. The die design for tube-hydroforming the front sub-frame was then investigated in the present study. Both the bending process and the perform design were optimized to avoid the presence of fracture. The proposed tube-hydroformed part design and the manufacturability of this part were validated by the production part. The consistency between the finite element simulation results and the production part in dimension accuracy confirms the effectiveness of the tube-hydroformed part design established in the present study.

Selection and peer-review under responsibility of the Department of Materials Science and Engineering, Nagoya University

Keywords: Hydroforming; Front sub-frame; Cross-section analysis; Strength

* Corresponding author. Tel.:+886-2-3366-2701; fax: +886-2-2363-1755.
E-mail address: fkchen@ntu.edu.tw

Selection and peer-review under responsibility of the Department of Materials Science and Engineering, Nagoya University
doi:10.1016/j.proeng.2014.10.308

1. Introduction

With the development of technology, the weight of vehicle body is also reduced. Among those technologies, tube-hydroforming is a well-known method to decrease the weight of vehicle body and this process can replace the original stamping part process design. Yoshida and others [1] have described the composition of front sub-frame and its functionality. Kim and others [2] have proposed front sub-frame process parameters design which include pressure and holder force. As for bending part, bending angle and radius as well as friction coefficient affect significantly on thinning [3, 4]. With respect to tube-hydroformed process, preforming design, friction coefficient and loading path will also affect product thinning [5-8] in the hydroforming process. Low-pressure forming process are discussed in the recent studies [9], which ultimate pressure is found to be limited by product radius [10, 11]. This Study aims to modify stamping part type design to tube-hydroformed part design, maintaining same static strength and dynamic strength.

2. Product cross-section analysis and design

2.1. Product introduction and cross-section analysis

This study has selected the front sub-frame of car front suspension system and mainly discusses the manufacturability and strength of modifying the original stamping part type design as tube-hydroformed part type in front sub-frame. The front sub-frame in stamping type is mainly welded by six stamping parts, four 2 mm stamping parts and two 3mm stamping parts, respectively.

This study modified the stamping type to the tube-hydroformed type. First, overall section expansion ratio in the stamping type was examined through the cross-section analysis. The result of cross-section analysis, as shown in Fig. 1, indicated that the maximum expansion ratio is about 72% in the port.

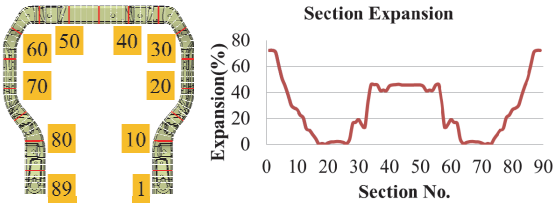

Fig. 1. Cut section and the section expansion.

2.2. Modification and design

Through the symmetric plane, this study divides product's feature region as port, side U and middle U. The maximum expansion ratios of port, side U, and middle U are 70%, 30% and 45%, respectively. The above results are shown in Fig. 2(a). Fig. 2(b) shows the modified concept design. This study enlarges the circumference of side U cross-section as about 20%. The result of modified tube-hydroformed type cross-section analysis shows in Fig. 2(c) and the maximum expansion ratio is about 29.36%.

After modifying product's surface, the overall maximum expansion decreased from 70% to about 30%, improving product's tube-hydroforming formability. In order to comply with the weight of stamping-welding parts of about 9.5kg, a circular tube with 2.5 mm thickness was selected to tube-hydroformed the front sub-frame.

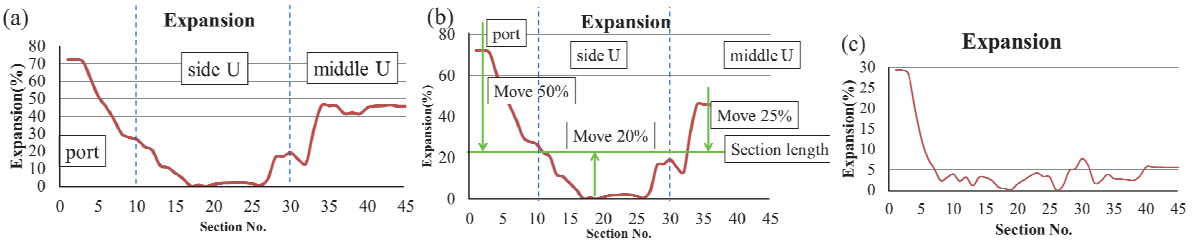

Fig. 2. Product expansion: (a) the result of cross-section analysis; (b) modified method; (c) cross-section analysis result for modified.

3. Front sub-frame formability and verification

3.1. Front sub-frame formability analysis

This study proposed the front sub-frame in tube-hydroformed type, and its formability was investigated. This front sub-frame is made of SPH440. Following the cross-section analysis, a tube of 65 mm in diameter was adopted for tube-hydroforming the front sub-frame. The tube-hydroforming process consists of three operations, including bending, preforming and tube-hydroforming. In order to facilitate the formability design, the commercial code PAM-STAMP was utilized to carry out the formability simulations. Fig. 3 shows that the product thinning after tube-hydroforming is 17%, and the maximum part-die mismatch distance is 1.74 mm.

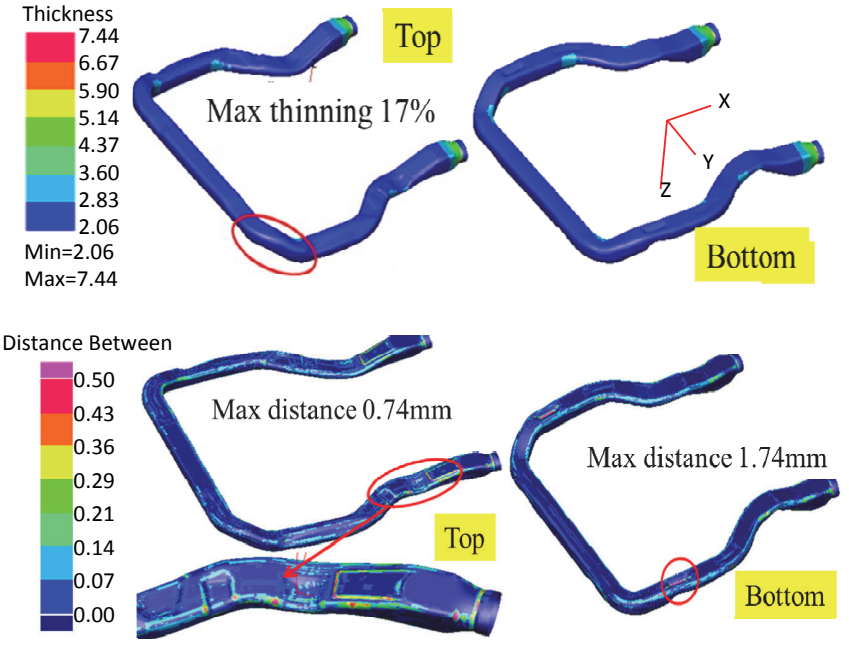

Fig. 3. Thinning result and distance result of CAE simulation.

3.2. Front sub-frame verification

In order to ensure correct FEM analysis result, this study employed ultrasonic thickness gauge to measure the product thickness. Fig. 4 displays middle U and port thickness measurement points. Table 1 shows the comparison

between the computed thickness and actual thickness in middle U. Table 2 gives the comparison between port simulated thickness and actual thickness. Therefore, this study draws a conclusion from these two tables that the computed thickness is approximate to actual thickness, which represents that the finite element simulations shaped on the tube-hydroforming process have considerable credibility.

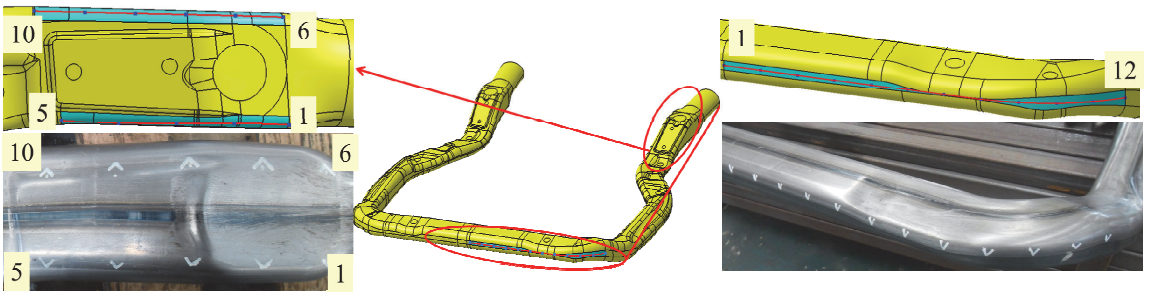

Fig. 4. Measure point position.

Table 1. The real thickness and the CAE result in the middle U.

Real thickness (mm)				CAE thickness(mm)			
No.	Thickness	No.	Thickness	No.	Thickness	No.	Thickness
1	2.39	7	2.68	1	2.39	7	2.56
2	2.39	8	2.29	2	2.38	8	2.15
3	2.42	9	2.03	3	2.39	9	2.12
4	2.39	10	1.99	4	2.36	10	2.07
5	2.45	11	2.12	5	2.47	11	2.13
6	2.72	12	2.40	6	2.58	12	2.41

Table 2. The real thickness and the CAE result in the port.

Real thickness (mm)				CAE thickness(mm)			
No.	Thickness	No.	Thickness	No.	Thickness	No.	Thickness
1	2.61	6	2.61	1	2.6	6	2.56
2	2.57	7	2.45	2	2.4	7	2.41
3	2.55	8	2.43	3	2.42	8	2.41
4	2.58	9	2.46	4	2.5	9	2.49
5	2.72	10	2.49	5	2.52	10	2.47

4. Static strength after product modification

4.1. Front sub-frame static model specification, simplification, and boundary condition

In the previous section, this study examines the formability of front sub-frame, and the strength of the designed part will be discussed in the following section. The static strength of the designed hydroformed part was investigated by comparing the stress and strain distributions of the part to those in the original stamping-welding parts when the engine is mounted on the front sub-frame. Besides front sub-frame itself, the main force structure also includes the engine-supported structure and structure part connecting front sub-frame and vehicle body. The rest structure parts are not considered.

Referring to the connection method of actual front sub-frame and vehicle body, the constraints were set on the part region marked in blue in both translation and rotation degree of freedoms, as shown in Fig. 5(a). In setting loading condition, this study considers the commercially available engine weight with 1900 N and loads the force at a point to simulate the front sub-frame strength when the engine is mounted. Fig. 5(b) shows the front sub-frame static boundary conditions.

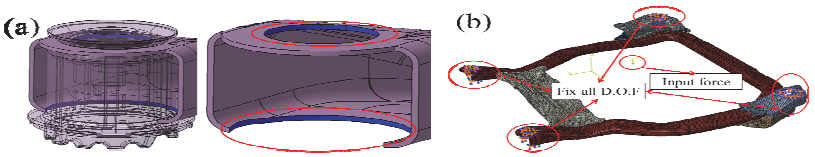

Fig. 5. Boundary condition: (a) port fixed position; (b) total boundary condition.

4.2. Static analysis result

From the simulation results of the static strength, we can know that tube-hydroformed type maximum stress is smaller than stamping type. Fig. 6(a) and Fig. 6(b) show respectively the stress distribution of stamping type and hydroformed type. From the result of displacement distribution, we can know that maximum displacement presents in the tube-hydroformed is a little larger than that presents in stamping type. It may be attributed to the thinner tube is used in the tube-hydroformed part. The sheet thickness of the middle U region in the stamping type is 3mm, while the tube-hydroformed type selects 2.5 mm in simulation. Fig. 7(a) and (b) displays respectively the displacement distributions of stamping type and tube-hydroformed type.

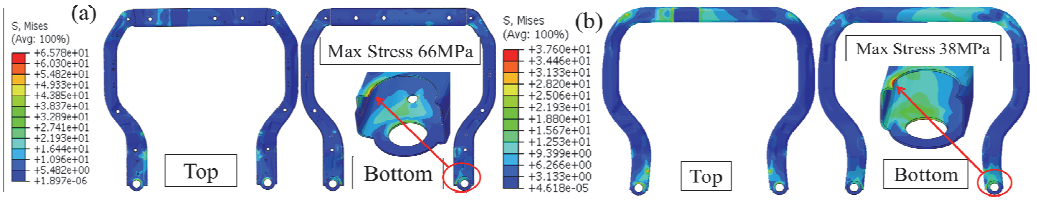

Fig. 6. Mises stress: (a) stamping type; (b) hydroformed type.

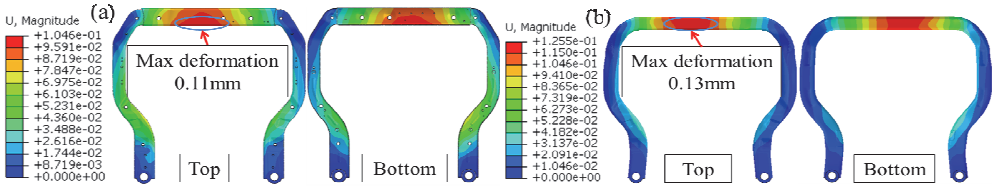

Fig. 7. Deformation: (a) stamping type; (b) hydroformed type.

5. Product dynamic intensity after modification

5.1. Front sub-frame dynamic model specification and simplification

This section shows the front sub-frame's impact test. The main factors that affect the deformation are structure parts and vehicle body that support engine. The remaining structure is not considered. This study used a cube to replace vehicle part, and its size decided by the input density parameters. The weight of general commercially available car is about 1500-2000 kg with the use of steel, and the steel density is 7850 kg/m^3. This study adopts HyperMesh to establish the mesh system with solid elements. Front sub-frame, the vehicle body and the supported engine structure are considered as a whole car. The vehicle hits the fixed wall with an overall speed of 60 km/hr.

5.2. The result of the dynamic analysis

The simulation results are shown in Fig. 8(a). As seen in Fig. 8(a), front sub-frame stamping type has the same deformation mechanism as tue-hydroformed type. In addition, this study also uses thickness 2.0 mm tube-hydroformed type to carry out impact analysis. Fig. 8(b) shows the energy absorbed in the impact. The absorbed energy of 2.5 mm tube-hydroformed type is better than 2.0 mm tube-hydroformed type, and the stamping-welding type being inferior to the tube-hydroformed part. As known from simulation results, the strength of the front sub-frame will be better if the thickness in the tube-hydroformed type is thicker.

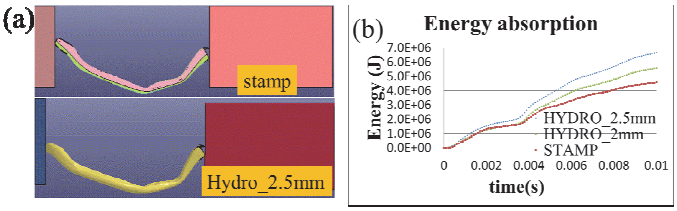

Fig. 8. Dynamic result: (a) crush phenomenon; (b) energy absorption.

6. Conclusion

Compared to traditional stamping product, the tube-hydroformed product has advantages of light weight and less production cost. This study has selected front sub-frame as the carrier to modify the stamping type to a one-piece tube tube-hydroformed type, conducting analysis on its strength and formability. This study has also established revised standard of which modifies stamping part type as tube-hydroformed part type design. First, we need to analyze product cross-section to understand the product in overall expansion ratio, and then consider the circumference design modification direction of product cross-section by expansion ratio. Followed by carrying out the part strength analysis using the finite element simulations, we may assure that the tube-hydroformed part meets the light weight and strength requirements.

The proposed tube-hydroformed part design and the manufacturability of this part were validated by the production part. The consistency between the finite element simulation results and the production part in dimension accuracy confirms the effectiveness of the tube-hydroformed part design established in the present study.

Furthermore, as known from the strength analysis results, stamping type and tube-hydroformed type exhibit similar trends under same load condition, including the stress and displacement distributions as well as the impact deformation mechanism. However, the strength capability and energy absorption of the tube-hydroformed front sub-frame are better than those exhibited in the stamping type, as shown in Table 3.

Table 3. The compared result between the stamping type and the hydroformed type.

	Stamping type	Hydroformed type
Weight	9.514(kg)	9.509(kg)
Number of Die	At least six	Up to two
Mises stress in static analysis	66(MPa)	38(MPa)
Deformation in static analysis	0.11(mm)	0.13(mm)
Energy absorption in dynamic analysis	$4.57*10^6$(J)	$6.66*10^6$(J)

Acknowledgements

The authors would thank the Unimax Group for providing the production part to validate the finite element analysis. They are also grateful to the ESI-France for the help in using the PAM_STAMP 2G program.

References

[1] Yoshida, H., 2002. Front sub-frame structure. U.S. Patent NO. 6390224.
[2] Kim, K. J., Kim, J. S., Choi, B. I., Kim, K. H., Choi, H. H., Kim, C. W., Kang, K. W., Song, J. H., Sung, C. W., 2007. Development of automotive engine cradle by hydroforming process. Journal of Mechanical Science and Technology 21, 1523-1527.
[3] Xu, X., Xiong, T., Guan, Q., Tan, L., 2012. Finite element simulation and numerical analysis in the process of tube bending. Advanced Materials Research 421, 14-18.
[4] Zhang, J., Li, F., Zhu, Q., Wang, Y., 2012. Research on process planning method of NC tube bending. Advanced Materials Research 411, 393-397.
[5] Lei, L. P., Kim, J., Kang, S. J., 2003. Rigid-plastic finite element analysis of hydroforming process and its applications. Journal of Materials Processing Technology 139, 187-194.
[6] Xu, X., Li, S., Zhang, W., Lin, Z., 2009. Analysis of thickness distribution of square-sectional hydroformed parts. Journal of Materials Processing Technology 209, 158-164.
[7] Gao, L., Motsch, S., Strano, M., 2002. Classification and analysis of tube hydroforming process with respect to adaptive FEM simulations. Journal of Materials Processing Technology 129, 261-267.
[8] Yang, J. B., Jeon, B. H., Oh, S. I., 2001. Design sensitivity analysis and optimization of the hydroforming process. Journal of Materials Processing Technology 113, 666-672.
[9] Nikhare, C., Weiss, M., Hodgson, P. D., 2010. Die closing force in low pressure tube hydroforming. Journal of Materials Processing Technology 210, 2238-2244.
[10] Hwang, Y. M., Lin, Y. K., Wu, H. C., Chen, H. C., 2001. FE-simulation on T-shape tube hydroforming, the 18th National Conference on Mechanical Engineering. Taipei, Taiwan R.O.C..
[11] Chen, F. K., 2003. Formability analysis of tube hydroforming process. Applied Mechanics and Engineering 4, 1, 149-169.